^{99m}Tc-HMPAO Regional Cerebral Blood Flow and Quantitative Electroencephalography in Alzheimer's Disease: A Correlative Study

Guido Rodriguez, Flavio Nobili, Francesco Copello, Paolo Vitali, Maria V. Gianelli, Gioconda Taddei, Elie Catsafados and Giuliano Mariani

Clinical Neurophysiology Service (Department of Internal Medicine, University of Genoa; Department of Organ Transplantation, S. Martino Hospital; and CNR Center for Cerebral Neurophysiology), Genoa; Institute of Occupational Medicine and Nuclear Medicine Service, Department of Internal Medicine, University of Genoa, Genoa, Italy

In this study the neuropsychological status of patients with Alzheimer's disease (AD) was correlated with quantitative electroencephalography (qEEG) and regional cerebral blood flow (rCBF) both in the cortex and in deep gray matter structures. **Methods:** Forty-three outpatients (mean age 72.4 ± 7.5 y) with probable AD underwent ^{99m}Tc-hexamethyl propyleneamine oxime SPECT with a brain-dedicated gamma camera and qEEG (relative values) within 1 mo. Preliminary factorial analysis with promax rotation identified four qEEG bands (2–5.5, 6–7.5, 8–11.5 and 12–22.5 Hz, with no distinction as to topography) and six SPECT regions (the two thalami together, the two parietal cortices together, the right temporal cortex, the right hippocampus, the left hippocampus and the remaining cortical areas together) as the variables with highest statistical power. All these variables and the Mini-Mental Status Examination score (MMSE, a sensitive marker of neuropsychological deficit) were processed by a final factorial analysis and multivariate analysis of variance. **Results:** Both the 2–5.5 Hz and the 8–11.5 Hz powers were correlated with the perfusion level in the parietal regions of interest (ROIs) (P = 0.0009), whereas the 2–5.5 Hz power was correlated with the right hippocampal perfusion level (P = 0.007). The MMSE score was significantly correlated with the perfusion level, both in the right (P = 0.006) and in the left (P = 0.004) hippocampal ROIs and in the parietal ROIs (P = 0.01); moreover, it was correlated with both the 2–5.5 Hz (P = 0.0005) and the 8–11.5 Hz (P = 0.004) power. **Conclusion:** rCBF (bilateral parietal perfusion) and qEEG (especially the slowest frequencies, i.e., 2–5.5 Hz) are confirmed to be good descriptors of AD severity. It is especially noteworthy that bilateral hippocampal CBF was the perfusional index best correlated with the MMSE as well as being significantly correlated to qEEG. Hippocampal SPECT imaging appears to be a promising index to improve characterization of AD in respect to other forms of primary degenerative dementia and may be proposed as a marker for evaluating the effects of pharmacotherapy of AD at the neuronal level.

Received Feb. 11, 1998; revision accepted Sep. 15, 1998.

For correspondence or reprints contact: Guido Rodriguez, MD, Clinical Neurophysiology Service, Department of Internal Medicine, University of Genova, Osp. Viale Benedetto xv, 6, I-16132 Genova, Italy.

Key Words: Alzheimer's disease; ^{99m}Tc-hexamethyl propyleneamine oxime SPECT; quantitative electroencephalogram

J Nucl Med 1999; 40:522–529

In patients with Alzheimer's disease (AD), the most typical perfusion deficits are usually found in the temporo-parieto-occipital or even the frontal associative cortex. Although cortical perfusion levels have been shown to correlate with surface electroencephalograms (EEGs), considerably less attention has been paid to the possible correlation between blood flow level in deep gray structures and EEG changes (*1–7*), notwithstanding the known involvement of some deep areas (such as the hippocampus) in the functional failure of AD patients, as ascertained by both pathologic (*8,9*) and MRI (*10*) studies. Moreover, the notion that the thalamus plays a definite role at least in the genesis of EEG background activity (*11*) raises questions about a possible relationship between surface EEG and thalamic regional cerebral blood flow (rCBF) in these patients.

We correlated the neuropsychological status of AD outpatients with quantitative EEG (qEEG) and cerebral perfusion in both superficial and deep gray structures, as assessed by a brain-dedicated, high-resolution SPECT camera and ^{99m}Tc-hexamethyl propyleneamine oxime (HMPAO).

MATERIALS AND METHODS

Patients

Fifty-five consecutive outpatients meeting the criteria of probable AD according to the definition of the National Institute of Neurological and Communicative Disorders and Stroke-Alzheimer's Disease and Related Disorders Association (NINCDS-ADRDA) work group (*12*) were eligible for this study. All patients had been referred to the Clinical Neurophysiology Service of our university by their general practitioners or by neurologists for first diagnostic screenings or to have the diagnoses confirmed. To rule out both secondary and mixed dementias, all patients underwent a complete diagnostic protocol, including general and neurological

examinations, basal and contrast-enhanced brain CT, duplex scanning of neck vessels, chest radiography, complete blood count, urinalysis, liver and kidney function tests, thyroid hormone assay, human immunodeficiency virus antibodies, Venereal Disease Research Laboratory slide test and B12 and folic acid assay. Alcohol abuse was ruled out by clinical history and by serum levels of alanine aminotransferase and gamma-glutamyltranspeptidase. Patients with CT signs of vascular lesions of any kind or white matter degeneration were excluded.

The presence of at least two cognitive deficits was documented by a detailed neuropsychological evaluation, including standard tests for orientation, memory, concentration and attention, abstraction and problem solving, language function, visual perception, visuoconstruction and praxis, as suggested by Morris et al. (*13*).

As part of the routine diagnostic procedure, patients also underwent qEEG and ^{99m}Tc-HMPAO SPECT.

From the original 55 patients, 12 were excluded because of (a) technically unsatisfactory brain SPECT (as the result of problems such as movement artifacts) (1 man, 2 women); (b) technically unreliable EEG traces (1 man, 4 women); and (c) an interval of more than 1 mo between the two examinations (3 men, 1 woman).

The remaining 43 patients (16 men, 27 women; age range 56–84 y, mean 72.42 ± 7.52 y) were enrolled in the study. Disease duration ranged from 12 to 132 mo (mean 48.5 ± 33.5 mo) and educational level from 1 to 15 y (mean 7.3 ± 3.4 y). Consistent with the diagnosis of AD, all patients scored lower than 4 on the Hachinski ischemic scale. The Global Deterioration Scale (GDS) (*14*) scored 3 and 4 for 10 patients each, 5 for 9 patients and 6 for 14 patients. On the Mini-Mental Status Examination (MMSE) (*15*) the score range was 1–24 (mean 15.07 ± 6.97). Forty patients were right-handed and 3 were left-handed (*16*).

^{99m}Tc-HMPAO SPECT

The SPECT equipment used in this study (CERASPECT; Digital Scintigraphics, Waltham, MA) acquires brain perfusion images of ^{99m}Tc-HMPAO by a camera equipped with a stationary NaI(Tl) annular crystal and an array of 63 photomultipliers built outside the crystal. The cylindrical-shaped, low-energy, high-resolution lead collimator is the only moving piece during the acquisition at 15 s/stop over 120 stops, with the head of the patient positioned inside. In this way the system optimizes the trade-off between spatial resolution and counting statistics. Sensitivity of the collimator with a point source in air is 190 cps/MBq (7.0 cps/μCi), with a spatial resolution for the 140 KeV of ^{99m}Tc < 8.5 mm at the center of rotation and 6.3 mm in peripheral regions (full width at half maximum). Geometry of the holes built in the collimator is equivalent to a three-head rotating gamma camera, in that three different regions of the detecting crystal contribute to acquisition of counts during each angular position. Dedicated hardware and software procedures average these three different sinograms into sinograms equivalent to those generated by a single-head camera (*17*).

All SPECT acquisitions were obtained between 30 and 90 min after intravenous injection of 740–925 MBq freshly-prepared ^{99m}Tc-HMPAO (Ceretec; Amersham Medical, Ltd., Amersham, UK). Sensory input was minimized while injecting the tracer in a quiet, dimly lit room, with the patient lying on a reclining chair (eyes closed and ears unplugged).

Sixty-four axial slices parallel to the cantho-meatal (CM) line, 1.67-mm thick, were reconstructed on a 128 × 128 matrix (1 pixel = 1.67 mm) using a two-dimensional Butterworth-filtered backprojection (cutoff 1 cm, order 10). The reconstructed images were corrected for attenuation with Chang's first-order method, applying an attenuation coefficient equal to 0.15/cm (*18*). Correction was also made for the nonlinear uptake of ^{99m}Tc-HMPAO with higher CBF values (*19*).

SPECT data analysis was performed on two transaxial sections. The first section (5-mm thick, 3 slices summed together) was chosen to identify as well as possible the hippocampal region (with the guidance of a widely used anatomic atlas [*20*]), including both the hippocampus and the hippocampal gyrus, after reorientation of the SPECT image on the sagittal plane, as suggested by Ohnishi et al. (*21*). Irregular and symmetrical regions of interest (ROIs) were hand drawn around the two hippocampal regions (Fig. 1, left). The

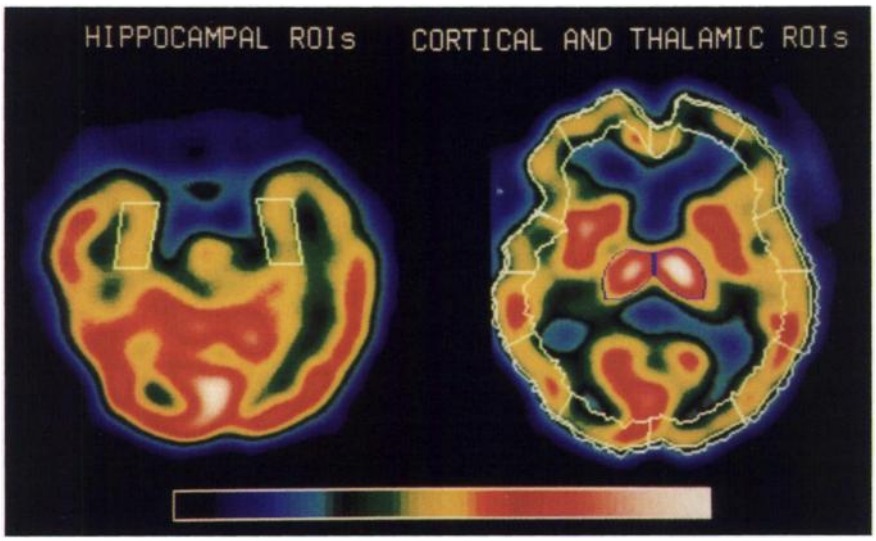

FIGURE 1. ^{99m}Tc-HMPAO SPECT. ROI drawings around hippocampi (left), in superficial cortex and around thalami (right). (Left) Reoriented transaxial section with two irregular but symmetrical ROIs around hippocampal region. (Right) Transaxial section parallel to CM line and crossing thalami with automatically drawn (cortical border) and hand-drawn (thalami) ROIs is shown. Common color scale is shown at bottom. Letter "L" indicates left cerebral hemisphere. Patient had mild AD (GDS = 3, MMSE score = 24).

second section (8.3-mm thick, 5 slices summed together) was constructed by summing up the 5 most intermediate of all the slices parallel to the CM line, which included the thalami. The outer cortical border was then automatically drawn by a software option at 30% of maximum counts of the summed 5-slice section, and the inner cortical border was drawn 1.67 cm (10 pixels × 1.67 mm) inside, as described by Mountz et al. (*22*). The cortical ribbon obtained in this way was then divided into 12 30° sectors in a clockwise fashion to identify 12 ROIs: 2 frontal, 2 temporal, 1 parietal and 1 occipital area in each hemisphere. In addition, irregular and symmetrical ROIs were hand drawn around the thalami (Fig. 1, right).

Normalization of SPECT data were obtained by computing ROI-to-cerebellar ratios (mean counts per pixel in each ROI over mean counts per pixel in the whole cerebellum). If a greater than 10% cerebellar asymmetry was found, the hemisphere with higher counts was considered as the reference region.

Quantitative Electroencephalography

EEG was recorded with each patient seated on a comfortable, high-backed chair in a quiet room, relaxed and awake with closed eyes, with constant control of vigilance level. The trace was recorded on paper for 30 min for conventional visual inspection by average reference from 16 scalp electrodes (ERA 21; OTE BIOMEDICA, Florence, Italy). Electrodes were positioned on Fp1, F3, C3, P3, O1, F7, T3, T5, Fp2, F4, C4, P4, O2, F8, T4 and T6, according to the 10–20 international system. Moreover, 5 min of EEG data were recorded on a computer and digitized at 128 Hz with a time constant of 0.1, high-frequency filter of 35 Hz and notch filter in each channel.

For quantitative analysis, 30 consecutive 2-s epochs free of artifacts were selected off line and processed by fast Fourier transform; the spectra obtained were then averaged to obtain a mean power spectrum (mPS) for each channel. As suggested by Buchan et al. (*23*), data below 2 Hz were excluded because of the large contribution from eye movement and blink artifacts. For each channel, the mPS was then divided into seven bands: 2–3.5 Hz (corresponding to the conventional Δ-2 band); 4–5.5 Hz (θ-1); 6–7.5 Hz (θ-2); 8–9.5 Hz (α-1); 10–11.5 Hz (α-2); 12–13.5 Hz (borderline frequencies between conventional α and β bands); and 14–22.5 Hz (β-1 and β-2). Figure 2 shows an example of mPS in a healthy control group in another study and in an AD patient.

The relative qEEG values were linearized by log transformation (log [x/(1 − x)]) for additional statistical analysis. The choice of relative qEEG values was based on data showing that they are able to express the electrophysiological derangement of AD with the same accuracy as absolute values (*24,25*) and that correlate more accurately to severity of dementia (*25*).

Statistics

The statistical analysis used in this study followed a multistep sequential approach that can be subdivided roughly into two phases. The scope of the preliminary phase was to reduce the number of variables under evaluation, initially too high to be handled efficiently. Similar statistical approaches have been applied to the original brain SPECT data with the purpose of identifying ROIs that contribute the most to the variance of the patient sample (*26–28*). In this study, the following sets of variables were available for each patient: (a) relative power of seven qEEG bands (2–3.5, 4–5.5, 6–7.5, 8–9.5, 10–11.5, 12–13.5, 14–22.5 Hz); (b) 16 EEG channels, each with its own distribution of the above

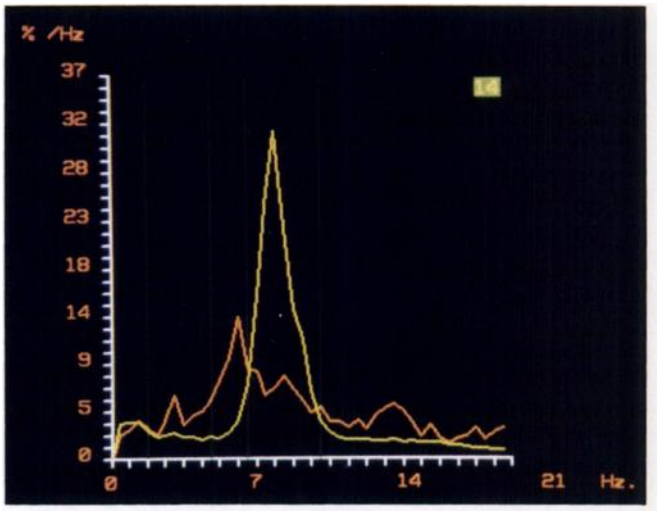

FIGURE 2. qEEG mean power spectrum in parietal channel of normal elderly group (yellow) and in same channel of patient (orange) with moderate AD (GDS = 5, MMSE score = 14). EEG frequency bands (x-axis: 2–5.5, 6–7.5, 8–11.5 and 12–22.5 Hz) and percent value of each band (y-axis) are shown. Normal group shows predominance of 8–11.5 Hz band power, whereas AD patient exhibits increase of both 6–7.5 Hz and 2–5.5 Hz band powers together with reduction of 8–11.5 Hz band power.

qEEG frequency bands; (c) 16 ROIs derived from the SPECT study (12 superficial cortical regions, 2 hippocampal regions and 2 thalamic ROIs, each characterized by a relative perfusion level); and (d) the MMSE score. Although the MMSE score is rather crude as a neuropsychological measure, it does summarize the neuropsychological deficit in a sensitive way and at the same time avoids an additional increase in the number of variables. As a result of this feature, MMSE is, in fact, often used for correlative purposes (*29*). Therefore, the sets of variables with highest statistical power (that is, those variables that best describe the variability observed in the group under study) were identified first.

This was achieved by sequential factorial analysis (two iterations generating five correlation axes) with promax rotation (Statistical Analysis System; SAS, Cary, NC) (*27,28,30*). This latter approach, often used in performing factorial analysis (*31–33*), first translates the correlation axes to make each statistical record as close as possible to the origin of the axes. Then the axes as a whole are translated so as to optimize distribution of each statistical record along each axis.

In the second phase, the set of variables, reduced to a minimum as described above, are subjected to a further factorial analysis and final multiple analysis of variance (MANOVA) to assess the relationships among the residual variables. To reduce type I error, the first level of significance for the correlation matrix was accepted as $P \leq 0.01$.

Finally, a principal component analysis was performed according to the method, described in detail elsewhere (*34,35*), to summarize in a graphical manner the results obtained from the correlation matrix of the MANOVA. This kind of analysis, part of the SAS package, has been used recently both in ^{99m}Tc-HMPAO SPECT studies (*26–28*) and in neuropsychological investigations (*36*) in patients with various cognitive disorders, including AD (*37*).

RESULTS

Preliminary Factorial Analysis

^{99m}Tc-HMPAO SPECT. Preliminary factorial analysis grouped all except the hippocampal ROIs (which were attributed to a fourth factor) in the second factor. Therefore, a supplementary, preliminary factorial analysis was performed on only all SPECT variables. This allowed the identification of six SPECT factors as statistically relevant: the right hippocampal ROI, the left hippocampal ROI, the right temporal ROI, the thalamic ROIs of both sides, the parietal ROIs of both sides and the remaining cortical ROIs together. A mean SPECT value was computed among the ROI ratios within each of the last three factors.

Quantitative EEG. Factorial analysis grouped the seven original qEEG bands into three factors. The first factor included both the 2–3.5 Hz and the 4.0–5.5 Hz bands and (with the opposite sign) both the 8–9.5 Hz and the 10–11.5 Hz bands; the second one included the 6–7.5 Hz band in addition to the SPECT variables; and the third factor grouped the 12–13.5 Hz and the 14–22.5 Hz bands. All 16 channels were always clustered together with the corresponding band within the same factor, thus indicating the poor topographic localization of EEG changes in AD. A mean value for each band across the 16 channels was then computed. The two mean values of the original narrow, adjacent bands within the same factor and with the same sign were averaged to form four final qEEG bands, i.e., three "new" wide bands (2–5.5, 8–11.5 and 12–22.5 Hz) and the original narrow 6–7.5 Hz band. Quantitative EEG variables were thus reduced from 112 per patient (7 band powers × 16 channels) to only 4 band powers per patient.

Final Factorial Analysis

For each patient, the 11 variables considered for the final factorial analysis were (a) the six SPECT ROIs (right hippocampus, left hippocampus, right temporal cortex, the two thalami, the two parietal cortices and all the other cortical regions); (b) the relative power of the four qEEG bands (2–5.5, 6–7.5, 8–11.5 and 12–22.5 Hz); and (c) the MMSE score.

The results of final factorial analysis are shown in Table 1. The first factor accounts for 42.2% of total variance and was made up of all the SPECT ROIs except for the hippocampal ones. The second factor accounts for 35% of total variance and included all the qEEG bands except the 6–7.5 Hz one. The third factor (accounting for 22.8% of total variance) was made up of the two hippocampal SPECT ROIs, the 6–7.5 Hz band and the MMSE score.

Multiple Analysis of Variance

The multivariate correlation matrix among the final 11 variables is shown in Table 2. A significant correlation was found between some of the SPECT and the qEEG variables, as follows: both the 2–5.5 Hz and the 8–11.5 Hz powers were correlated with perfusion level in the parietal ROIs ($P = 0.0009$), whereas the 2–5.5 Hz power was correlated with perfusion level in the right hippocampal ROI ($P = 0.007$). A weaker (borderline) correlation was found between both the 8–11.5 Hz and the 12–22.5 Hz power and perfusion level in the right hippocampal ROI ($P < 0.05$). Similarly, a borderline correlation was observed between the 2–5.5 Hz power and perfusion level in the right temporal ROI ($P = 0.05$).

TABLE 1
Factorial Analysis with Promax Rotation on Quantitative Electroencephalography, SPECT Variables, and Mini-Mental Status Examination (MMSE)

	Factor 1*	Factor 2*	Factor 3*
MMSE	0.01020	0.23143	0.56476
2–5.5 Hz relative power	−0.00182	−0.98399	−0.00907
6–7.5 Hz relative power	−0.00050	−0.09115	0.88583
8–11.5 Hz relative power	0.00051	1	0.00843
12–22.5 Hz relative power	0.00094	0.93032	−0.02685
R hippocampal rCBF	0.12063	0.10751	0.49425
L hippocampal rCBF	0.04102	0.00202	1
Thalamic rCBF	1	−0.00098	0.00009
R temporal rCBF	0.92336	0.00838	0.00428
Parietal rCBF	0.88515	0.01530	0.00625
rCBF in the remaining cortex	0.91642	0.00076	0.01780

*Factorial weights are shown.
R = right; rCBF = regional cerebral blood flow; L = left.

The MMSE score was significantly correlated to some of the qEEG and the SPECT variables, as follows: with the right ($P = 0.006$) and the left ($P = 0.004$) hippocampal rCBF, and with the parietal ($P = 0.01$) rCBF; with the 2–5.5 Hz ($P = 0.0005$) and the 8–11.5 Hz ($P = 0.004$) power. A weaker correlation ($P = 0.04$) was found between MMSE and perfusion of the cortical ROIs grouped together.

A graphic representation of the relationships among these 11 final variables is given in Figure 3, in which the results of principal component analysis are shown. The results were plotted on the first factorial plane, where the cosine of the angle at the center between two variables corresponds to the correlation coefficient, r^2.

DISCUSSION

Quantitative Electroencephalography

All 16 channels were pooled in the same factor as the respective frequency band. Therefore, topography of EEG changes does not seem to bear any relevant information in this sample of AD patients, consistent with other investigations using different statistical analyses (*5*). The issue of poor topographical localization of EEG abnormalities in AD patients, in spite of rather focal blood flow and metabolism changes observed by SPECT and PET techniques (*38*), remains unanswered as yet.

The set of qEEG frequencies identified by the preliminary

TABLE 2
Correlation Matrix (Multiple Analysis of Variance) Between Qualitative Electroencephalography (Columns), SPECT Variables (Rows) and MMSE

	MMSE	2–5.5 Hz relative power	6–7.5 Hz relative power	8–11.5 relative power	12–22.5 relative power
		r = **−0.5102**	0.0290	**0.4347**	0.0301
MMSE	1	P = **0.0005**	0.8938	**0.0036**	0.8481
R hippocam	**0.4114**	**−0.4037**	0.1600	**0.3016**	**0.3274**
rCBF	**0.0061**	**0.0073**	0.3053	**0.0494**	**0.0321**
L hippocam	**0.4330**	−0.2381	0.2538	0.1850	0.0187
rCBF	**0.0037**	0.1241	0.1006	0.235	0.9053
Thalamic	0.1826	−0.0535	−0.0075	−0.009	0.0053
rCBF	0.2411	0.7329	0.9617	0.9541	0.9733
R temporal	0.2600	−0.2975	0.0241	0.2565	0.1690
rCBF	0.0922	0.0527	0.8782	0.0968	0.2787
Parietal	**0.3883**	**−0.4879**	0.1209	**0.4872**	0.1118
rCBF	**0.0101**	**0.0009**	0.4399	**0.0009**	0.4754
Other cortic	**0.3117**	−0.2367	0.0611	0.1979	0.0893
rCBF	**0.0419**	0.1264	0.6969	0.2032	0.5688

MMSE = Mini-Mental Status Examination; rCBF = regional cerebral blood flow; R = right; L = left; hippocam = hippocampus; other cortic = cortical rCBF other than indicated above.

All correlations with a P value < 0.05 are in **bold.** For the sake of simplicity, complete definition of the statistical parameters (r and P) is given in the top cell of the first column.

factorial analysis matches other EEG findings in AD. In fact, the slow frequencies up to 5.5 Hz were clustered in the same factor as a pooled expression of EEG slowing, with a similar spectrum boundary as that used in other studies (*25,39,40*). This band power was highly and inversely correlated with the MMSE score, in substantial agreement with the correlation found between MMSE and similar indices of qEEG slowing reported by other authors (*25,41,42*). Also, the inverse correlation between the 2–5.5 Hz power and bilateral parietal rCBF is in keeping with the findings of other studies performed with ^{133}Xe for rCBF (*7*), or with [^{18}F] fluorodeoxuglucose PET for glucose metabolism (*43*).

Therefore, EEG slow frequencies are confirmed to be a good marker of the severity of AD by strictly reflecting bilateral parietal hypoperfusion and, indirectly, cerebral metabolic failure. The correlation of this slow qEEG band power with the right hippocampal rCBF (which was also significantly correlated with the MMSE score) is somewhat more intriguing. It is hypothesized that the human hippocampus is characterized by EEG frequencies between 4 and 7 Hz, as in most mammals evaluated by stereo-EEG (*11*). Indeed, hippocampal nuclei of some epileptic patients were shown to generate frequencies as low as 3 Hz (*44*). These frequencies partially overlap the slow band identified in this study (2–5.5 Hz). Therefore, it might be speculated that hippocampal EEG activity has affected surface EEG recording to some extent. Because the hippocampus (one of the key structures of memory) is involved early in AD (*10*), the relationships linking the degree of hypoperfusion, EEG slowing and cognitive performances (as expressed by the MMSE score) could then be explained. The discrepancy in the significance of correlation of the right (highly significant) and the left (poorly significant) hippocampal regions with the other variables will be addressed later in this article.

A thin area of the spectrum, namely the 6–7.5 Hz band, was isolated from the other qEEG bands, both in the preliminary and in the final factorial analysis and, moreover, was not correlated to either the MMSE score or any SPECT data. This may be the consequence of the statistical approach applied here, possibly isolating those spectral components that could worsen the result of the model as a whole. This model was essentially represented by a two-pole configuration (Fig. 3), with the 2–5.5 Hz factor in an opposite position to the 8–11.5 Hz factor and (to a lesser extent) to the 12–22.5 Hz factor. Indeed, the 6–7.5 Hz band may be ambiguous in this sample of AD patients with widely differing severity of disease. Such relatively low frequencies can simply represent the overall slowing of background EEG activity in early AD; on the other hand, they may represent the more organized θ frequencies usually observed later in the course of the disease. Thus, the same pattern may actually express very different pathophysiologic phenomena. This may explain the isolation of these frequencies from the statistical model and the lack of correlation with rCBF and cognitive performances.

The 8–11.5 Hz band (the dominant background frequencies) had an opposite position with respect to the 2–5.5 Hz band, a somewhat expected result since relative rather than absolute power values were considered in this study. Also the correlations (obviously with an opposite sign) with the other variables were very similar.

With the exception of a weak correlation with right hippocampal rCBF, the 12–22.5 Hz band did not show any significant correlation with either the MMSE score or the rCBF data, in agreement with the majority of previous reports (*7,43,45,46*).

^{99m}Tc-HMPAO SPECT

Pooling almost all the SPECT ROIs (except the two hippocampal ROIs) in the same factor and the high correlation indices within all the ROIs ($0.67 < r < 0.87$; data not shown) point to the high interdependence of the perfusion level in several areas in the same patient, as already shown by a prior study using the ^{133}Xe technique for rCBF evaluation (*47*). Ad hoc factorial analysis focused only on the SPECT data led to the identification of the bilateral parietal, right temporal, left hippocampal, right hippocampal and bilateral thalamic ROIs as separate factors from all the other cortical ROIs.

Thalamic perfusion did not correlate with either the MMSE score or qEEG variables. This lack of correlation may be explained by taking into account the fact that the thalami are substantially spared from the pathological process (*48–50*), whereas the related cortical fields generating EEG are involved to various extents. Therefore, the slow EEG activities generated within a deranged cortex bear poor

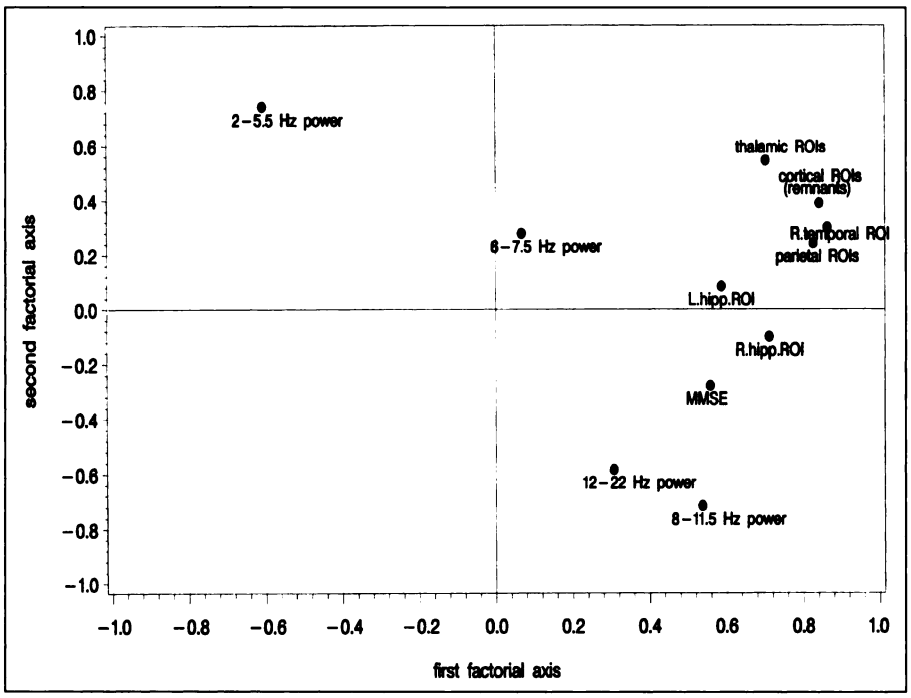

FIGURE 3. Graphical representation of relationships among 11 final variables by principal component analysis. Both x-axis and y-axis show factorial weight of each variable. Cosine of angle between two variables corresponds to correlation coefficient r^2. 0° angle (cos = 1) represents highest direct correlation, whereas 180° angle (cos = −1) corresponds to highest inverse correlation. 90° angle (cos = 0) is equivalent to no correlation at all.

correlation with otherwise spared and apparently functioning thalamic nuclei.

The bilateral parietal perfusion level was related to both the severity of disease and qEEG. This finding is in keeping with a recent PET study that showed the significant correlation between an index of qEEG slowing and cerebral metabolic rate for oxygen in temporo-parietal regions, especially in the left hemisphere (LH), in AD patients (*23*).

Interestingly, both hippocampal ROIs were significantly related to the MMSE score, a finding that emphasizes the sensitivity of SPECT in detecting the functional impairment of this structure, which is so relevant in determining the clinical deficit. The assessment of hippocampal perfusion by SPECT seems therefore crucial both in diagnosing and staging AD patients, as suggested also by the data of Ohnishi et al. (*21*), who reported that the hippocampal perfusion level assessed by ^{99m}Tc-HMPAO SPECT discriminated AD patients from healthy controls better than the parietal perfusion level. Our findings are somewhat consistent with the observation of Ohnishi et al. and also provide a more stringent statistical correlation between right hippocampal perfusion and both qEEG evaluation and a neuropsychological score (the MMSE).

The correlations found between both hippocampal and temporal perfusion and qEEG were significant in the right hemisphere (RH) only. The exact pathophysiologic meaning of such a side-related difference is not clear as yet. In a qEEG/rCBF asymmetry study (*4*), a significant correlation was reported in a group of 20 AD patients between mean hemispheric α-band power and rCBF (^{133}Xe SPECT) asymmetries. These authors found a predominant impairment of the LH in younger and mildly demented patients, and of the RH in older (>65 y) and more severely demented patients. However, the prevalence of impairment either in RH or in LH in relation to presenile or senile AD and to the severity of AD is still debated. Indeed, although several reports confirm the prevalence of LH impairment in presenile AD (*45,51–54*) and of RH impairment in senile AD (*4,41,55*), other investigations do not agree with this conclusion (*48,56*). Our patient group included a great majority of older patients (36 of 43 older than 65 y) and showed a predominance of RH impairment (17 of 20 patients with a greater than 5% hemispheric rCBF asymmetry had lower rCBF in the RH, data not shown) without correlation between asymmetries and MMSE score. This might explain the closer correlation we found in the RH between qEEG and rCBF and seems to support the view that in older AD patients the impairment of the RH is more frequent, irrespective of the severity of disease. Indeed, in previous studies in mainly senile AD, right temporo-parietal qEEG and ^{133}Xe rCBF values discriminated between AD patients and healthy controls (*57*) or, using qEEG data only, predicted the timing of evolution of AD better than the corresponding left values (*58*).

The issue of possible pathological asymmetries in AD is intriguing but not clarified as yet. The few pathological studies addressing this issue have actually found asymmetries in the density of both senile plaques and neurofibrillary tangles in several brain regions, including the superior temporal cortex and the hippocampus but without any prevalence of impairment in one hemisphere over the other

(*59*). However, some anatomic data seem to suggest that the right structures may be smaller than the left. In fact, the right planum temporale has been shown to be smaller than the left in humans (*60*), and it has been reported recently that, in an MRI study, the right hippocampal region is smaller than the left in normal subjects carrying the apolipoprotein E epsilon4 allele (frequently found also in AD patients) but not in those without such a feature (*61*). Therefore, there may be either premorbid or genetic anatomic reasons accounting for correlation asymmetries of the kind found in this study and in others (*4,41,45,48,51–58*).

CONCLUSION

The findings of this study emphasize the relevance of a methodologically sound neurophysiological approach (such as ^{99m}Tc-HMPAO SPECT and qEEG) to AD patients. In particular, ^{99m}Tc-HMPAO SPECT of the hippocampal region appears to be a sensitive tool in assessing both the clinical deficit and the electrophysiologic derangement, even better than parietal rCBF. Moreover, although intrinsically semiquantitative in nature, relative rCBF values estimated by ^{99m}Tc-HMPAO SPECT proved to be highly correlated with more quantitative estimates of metabolic derangement, such as those provided by qEEG. This was true not only for superficial, cortical layers of gray matter but also for deep gray structures, such as the hippocampal regions. The widely available brain SPECT examination versus the more limited availability of PET evaluation may therefore have a key role in staging disease severity.

The significant relationships of both SPECT and qEEG with a sensitive parameter (the MMSE score) of even mild neuropsychological changes during AD should stimulate wider use of these procedures as reliable tools in assessing the impact of drug therapy on neuronal function in AD patients. In this perspective, rCBF improvement has been shown after the administration of cholinergic agents, such as physostigmine (*62*), linopirdine (*63*) and velnacrine (*64*). Similarly, a reduction of slow frequency power induced by the administration of nerve growth factor (*65*) and tacrine (*66*) has been reported by qEEG, whereas lecithin was proven to have no such effects (*67*).

Finally, the data on hippocampal perfusion seem especially promising. Indeed, two potential directions for the proficient use of SPECT hippocampal findings in AD may be identified. The first concerns differential diagnosis: Although parietotemporal hypoperfusion is a reliable marker of AD in comparison with both frontotemporal dementia and the patched hypoperfusion of vascular dementia, the cortical hypoperfusion pattern does not have the same accuracy in distinguishing between AD and other forms of primary dementia, such as the Lewy body disease (*68*). An ad hoc study should be planned to verify whether the assessment of hippocampal rCBF adds relevant information to this aim. The second is the use of SPECT hippocampal perfusion level as a marker of the effects of pharmacotherapy in AD, as recently suggested by Lawrence and Sahakian (*69*). In fact, the hippocampus is regarded as a carrefour of many neurotransmitter pathways, including the cholinergic one (*70*), because of its peculiar neuronal networks. Therefore, a future line of research would be to test hippocampal SPECT imaging as a reliable marker of the effects of drugs acting on neurotransmission.

ACKNOWLEDGMENT

This study was supported in part by the project BIOMED-2 S.I.D., proposal no. PL-96–3130.

REFERENCES

1. Joannesson G, Brun A, Gustafson I, Ingvar DH. EEG in presenile dementia related to cerebral blood flow and autopsy findings. *Acta Neurol Scand.* 1977;56:89–103.
2. Sheridan PH, Sato S, Foster N, et al. Relation of EEG alpha background to parietal lobe function in Alzheimer's disease as measured by positron emission tomography and psychometry. *Neurology.* 1988;38:747–750.
3. Ihl R, Eilles C, Frolich L, Maurer K, Dierks T, Persic I. Electrical brain activity and cerebral blood flow in dementia of the Alzheimer type. *Psychiatry Res.* 1989;29:449–452.
4. Celsis P, Agniel A, Le Tinnier A, et al. Lateral asymmetries in primary degenerative dementia of the Alzheimer type. A correlative study of cognitive, hemodynamic and EEG data, in relation with severity, age of onset and sex. *Cortex.* 1990;26:585–596.
5. Szelies B, Grond M, Herholz K, Kessler J, Wullen T, Heiss WD. Quantitative EEG mapping and PET in Alzheimer's disease. *J Neurol Sci.* 1992;110:46–56.
6. Sloan EP, Fenton GW, Kennedy NSJ, MacLennan JM. Electroencephalography and single photon emission computed tomography in dementia: a comparative study. *Psychol Med.* 1995;25:631–638.
7. Passero S, Rocchi R, Vatti G, Burgalassi L, Battistini N. Quantitative EEG mapping, regional cerebral blood flow, and neuropsychological function in Alzheimer's disease. *Dementia.* 1995;6:148–156.
8. Hyman BT, Van Hoesen GW, Damasio AR. Memory-related neural system in Alzheimer's disease: an anatomic study. *Neurology.* 1990;40:1721–1730.
9. Arriagada PV, Growdon JH, Hedley Whyte ET, Hyman BT. Neurofibrillary tangles but not senile plaques parallel duration and severity of Alzheimer's disease. *Neurology.* 1992;42:631–639.
10. Ikeda M, Tanabe H, Nakagawa Y, et al. MRI-based quantitative assessment of the hippocampal region in very mild to moderate Alzheimer's disease. *Neuroradiology.* 1994;36:7–10.
11. Steriade M, Gloor P, Llinàs RR, Lopes da Silva FH, Mesulam M-M. Basic mechanisms of cerebral rhythmic activities. *Electroenceph Clin Neurophysiol.* 1990;76:481–508.
12. McKhann G, Drachman D, Folstein M, Katzman R, Price D, Stadlan EM. Clinical diagnosis of Alzheimer's disease: report of the NINCDS-ADRDA Work Group under the auspices of Department of Health and Human Services Task Force on Alzheimer's disease. *Neurology.* 1984;34:939–944.
13. Morris JC, Heyman A, Mohs RC, CERAD Investigators. The consortium to establish a registry for Alzheimer's disease. Part I. Clinical and neuropsychological assessment of Alzheimer's disease. *Neurology.*1989;39:1159–1165.
14. Reisberg B, Ferris SH, De Leon MJ, Crook T. The global deterioration scale for assessment of primary degenerative dementia. *Am J Psychiatry.* 1982;139:1136–1139.
15. Folstein MF, Folstein SE, McHugh PR. "Mini Mental State": a practical method for grading the cognitive state of patients for the clinician. *J Psychiatry Res.* 1975;12:189–198.
16. Oldfield RC. The assessment and analysis of handedness: the Edinburgh inventory. *Neuropsychologia.* 1970;9:97–113.
17. Genna S, Smith AP. The development of ASPECT, an annular single crystal brain camera for high efficiency SPECT. *IEEE Trans Nucl Sci.* 1988;35:654–658.
18. Chang, LT. A method for attenuation correction in radionuclide computed tomography. *IEEE Trans Nucl Sci.* 1978; 25:638–643.
19. Lassen NA, Anderson AR, Friberg L, Paulson OB. The retention of ^{99m}Tc-d,l-HMPAO in the human brain after intracarotid bolus injection: a kinetic analysis. *J Cereb Blood Flow Metab.* 1988;8:S13-S22.
20. Talairach J, Tournoux P. *Co-planar Stereotaxic Atlas of the Human Brain.* New York, NY: Thieme Medical Publishers, Inc.; 1980.
21. Ohnishi T, Hoshi H, Nagamachi S, et al. High-resolution SPECT to assess hippocampal perfusion in neuropsychiatric diseases. *J Nucl Med.* 1995;36:1163–1169.

22. Mountz JM, Deutsch G, Kuzniecky R, et al. Brain SPECT: 1994 update. In: Freemen LM, ed. *Nuclear Medicine Annual.* New York, NY: Raven Press; 1994:1–54.
23. Buchan RJ, Nagata K, Yokoyama E, et al. Regional correlations between the EEG and oxygen metabolism in dementia of Alzheimer's type. *Electroenceph Clin Neurophysiol.* 1997;103:409–417.
24. Soininen H, Partanen J, Paakkonen A, Koivisto E, Riekkinen PJ. Changes in absolute power values of EEG spectra in the follow-up of Alzheimer's disease. *Acta Neurol Scand.* 1991;83:133–136.
25. Leuchter AF, Cook IA, Newton TF, et al. Regional differences in brain electrical activity in dementia: use of spectral power and spectral ratio measures. *Electroenceph Clin Neurophysiol.* 1993;87:385–393.
26. Strother S, Kanno I, Rottenberg D. Principal component analysis, variance partitioning and "functional connectivity." *J Cereb Blood Flow Metab.* 1995;15: 353–360.
27. Houston A, Kemp P, MacLeod M. A method for assessing the significance of abnormalities in HMPAO SPECT. *J Nucl Med.* 1994;35:239–244.
28. Jones K, Johnson KA, Becker A, Spiers PA, Albert MS, Holman BL. Use of singular value decomposition to characterize age and gender differences in SPECT cerebral perfusion. *J Nucl Med.* 1998;39:965–973.
29. Peskind ER, Leverenz J, Farlow MR, et al. Clinicopathologic correlations of soluble amyloid beta-protein precursor in cerebrospinal fluid in patients with Alzheimer disease and controls. *Alzheimer Dis Assoc Disord.* 1997;11:201–206.
30. Cureton EE, Mulaik SA. The weighted varimax rotation and the promax rotation. *Psychometrika.* 1975;40:183–195.
31. Bagley CR. Factor structure of temperament in the third year of life. *J Gen Psychol.* 1991;11:291–297.
32. Ramsay MC, Reynolds CR. Separate digits tests: a brief history, a literature review, and a reexamination of the factor structure of the test of memory and learning (TOMAL). *Neuropsychol Rev.* 1995;5:151–171.
33. Craighead WE, Evans DD. Factor analysis of the Montgomery-Asberg depression rating scale. *Depression.* 1996;4:31–33.
34. Morrison DF. *Multivariate Statistical Methods.* 2nd ed. New York, NY: McGraw-Hill Book Co.; 1976.
35. Armitage P, Berry G. *Statistical Methods in Medical Research.* 2nd ed. Oxford, UK: Blackwell Scientific Publications; 1987:327–333.
36. Boles DB. Relationships among multiple task asymmetries. *Brain Cogn.* 1998;36: 268–289.
37. Strite D, Massman PJ, Cooke N, Doody RS. Neuropsychological asymmetries in Alzheimer's disease: verbal versus visuoconstructional deficits across stages of dementia. *J Int Neuropsychol Soc.* 1997;3:420–427.
38. Messa C, Fazio F, Costa DC, Ell PJ. Clinical brain radionuclide imaging studies. *Semin Nucl Med.* 1995;25:111–143.
39. Rosadini G, Cogorno P, Marenco S, Nobili F, Rodriguez G. Brain functional imaging in senile psychopathology. *Int J Psychophysiol.* 1991;10:271–280.
40. Signorino M, Pucci E, Belardinelli N, Nolfe G, Angeleri F. EEG spectral analysis in vascular and Alzheimer dementia. *Electroenceph Clin Neurophysiol.* 1995;94: 313–325.
41. Brenner RP, Ulrich RF, Spiker DG, et al. Computerized EEG spectral analysis in elderly normal, demented and depressed subjects. *Electroenceph Clin Neurophysiol.* 1986;64:483–492.
42. Primavera A, Novello P, Finocchi C, Canevari E, Corsello L. Correlation between Mini-Mental State Examination and quantitative electroencephalography in senile dementia of Alzheimer type. *Neuropsychobiol.* 1990;23:74–78.
43. Szelies B, Grond M, Herholz K, Heiss W-D. Functional disturbance in Alzheimer's dementia: EEG power mapping versus PET of glucose metabolism [abstract]. *J Cereb Blood Flow Metab.* 1991;11(suppl):S169.
44. Arnolds DEAT, Lopes da Silva FH, Aitink JW, Kamp A, Boeijinga P. The spectral properties of hippocampal EEG related to behavior in man. *Electroenceph Clin Neurphysiol.* 1980;50:324–328.
45. Schreiter-Gasser U, Gasser Th, Ziegler P. Quantitative EEG-analysis in early onset Alzheimer's disease: correlations with severity, clinical characteristcs, visual EEG and CCT. *Electroenceph Clin Neurophysiol.* 1994;90:267–272.
46. Muller TJ, Strik WK, Thome J, et al. Comparative studies in Alzheimer's disease: electroencephalographic brain mapping, HMPAO-SPECT and psychometric tests [abstract]. *Hum Brain Mapping.* 1995;1(suppl):392.
47. Blauenstein UW, Halsey JS, Wilson EM, Wills EL, Risberg J. 133-xenon method, analysis of reproducibility: some of its physiological implications. *Stroke.* 1977;8:92–102.
48. Deutsch G, Tweedy J. Cerebral blood flow in severity-matched Alzheimer and multi-infarct patients. *Neurology.* 1987;37:431–438.
49. Perani D, Di Piero V, Vallar G, et al. Technetium-99m HM-PAO-SPECT study of regional cerebral perfusion in early Alzheimer's disease. *J Nucl Med.* 1988;29: 1507–1514.
50. O'Brien JT, Eagger S, Syed GMS, Sahakian BJ, Levy R. A study of regional cerebral blood flow and cognitive performance in Alzheimer's disease. *J Neurol Neurosurg Psychiatry.* 1992;55:1182–1187.
51. Stefoski D, Bergen D, Fox J, Morrell F, Huckman M, Ramsey R. Correlation between diffuse EEG abnormalities and cerebral atrophy in senile dementia. *J Neurol Neurosurg Psychiatry.* 1976;39:751–755.
52. Small GW, Kuhl DE, Riege WH, et al. Cerebral glucose metabolic patterns in Alzheimer's disease. *Arch Gen Psychiatry.* 1989;46:527–532.
53. Schreiter-Gasser U, Gasser Th, Ziegler P. Quantitative EEG-analysis in early onset Alzheimer's disease: a controlled study. *Electroenceph Clin Neurophysiol.* 1993;86:15–22.
54. d'Onofrio F, Salvia S, Petretta V, Bonavita V, Rodriguez G, Tedeschi G. Quantified EEG in normal aging and dementias. *Acta Neurol Scand.* 1996;93:336–345.
55. Jagust WJ, Reed BR, Seab JP, Budinger TF. Alzheimer's disease. Age of onset and single-photon emission computed tomographic patterns of regional cerebral blood flow. *Arch Neurol.* 1990;47:628–633.
56. Duffy FH, Albert MS, McAnulty GB. Brain electrical activity in patients with presenile and senile dementia of Alzheimer's type. *Ann Neurol.* 1984;16:439–448.
57. Rodriguez G, Nobili F, Rocca G, De Carli F, Gianelli MV, Rosadini G. Quantitative electroencephalography and regional cerebral blood flow: discriminant analysis between Alzheimer's patients and healthy controls. *Dementia Geriatr Cogn Disord.* 1998;9:274–283.
58. Rodriguez G, Nobili F, Arrigo A, et al. Prognostic significance of quantitative electroencephalography in Alzheimer patients: preliminary observations. *Electroenceph Clin Neurophysiol.* 1996;99:123–128.
59. Moossy J, Zubenko GS, Martinez AJ, Rao GR, Kopp U, Hanin I. Lateralization of brain morphologic and cholinergic abnormalities in Alzheimer's disease. *Arch Neurol.* 1989;46:639–642.
60. Galaburda AM. Asymmetries of cerebral neuroanatomy. *Ciba Fund Symp.* 1991;162:219–233.
61. Tohgi H, Takahashi S, Kato E, et al. Reduced size of right hippocampus in 39- to 80-year-old normal subjects carrying the apolipoprotein E epsilon4 allele. *Neurosci Lett.* 1997;236:21–24.
62. Hunter R, Wyper DJ, Patterson J, Hansen MT, Goodwin GM. Cerebral pharmacodynamics of physostigmine in Alzheimer's disease investigated using single-photon computerised tomography. *Br J Psychiatry.* 1991;158:351–357.
63. van Dyck CH, Lin CH, Robinson R, et al. The acetylcholine releaser linopirdine increases parietal regional cerebral blood flow in Alzheimer's disease. *Psychopharmacology.* 1997;132:217–226.
64. Siegfried KR. Pharmacodynamic and early clinical studies with velnacrine. *Acta Neurol Scand.* 1993;149(suppl):26–28.
65. Lapchak PA. Nerve growth factor pharmacology: application to the treatment of cholinergic neurodegeneration in Alzheimer's disease. *Exp Neurol.* 1993;124: 16–20.
66. Riekkinen P Jr, Riekkinen M, Fisher A, Ekonsalo T, Sirvio J. Effects of muscarinic receptor agonists and anticholinesterase drugs on high voltage spindles and slow waves. *Eur J Pharmacol.* 1993;10:240:1–7.
67. Duffy FH, McAnulty G, Albert M, Durwen H, Weintraub S. Lecithin: absence of neurophysiologic effect in Alzheimer's disease by EEG topography. *Neurology.* 1987;37:1015–1019.
68. Talbot PR, Lloyd JJ, Snowden JS, Neary D, Testa HJ. A clinical role for ^{99m}Tc-HMPAO SPECT in the investigation of dementia? *J Neurol Neurosurg Psychiatry.* 1998;64:306–313.
69. Lawrence AD, Sahakian BJ. The cognitive psychopharmacology of Alzheimer's disease: focus on cholinergic systems. *Neurochem Res.* 1998;23:787–794.
70. Parra P, Gulyas AI, Miles R. How many subtypes of inhibitory cells in the hippocampus? *Neuron.* 1998;20:983–993.